Electronic theory of ordering and segregation in transition-metal alloys

Mark O. Robbins* and L. M. Falicov
Physics Department, University of California, Berkeley, California 94720
(Received 20 July 1983; revised manuscript received 26 October 1983)

A model for the electronic energy of alloys with arbitrary composition and short-range order is applied to 4*d* transition metals. The model is not *ab initio*, but only requires information about pure elemental properties which is readily available. A model Hamiltonian for the alloy is derived from these elemental properties. The electronic density of states and heat of formation are calculated from the Hamiltonian with the alloy cluster-Bethe-lattice method. Charge transfer is treated self-consistently. Results for the twenty-eight 4*d* transition-metal alloys are compared to experiment and other calculations. Predictions for the stable phase at zero temperature are in excellent agreement with experiment. The model calculation allows us to examine the physical basis for experimental trends.

I. INTRODUCTION

Transition-metal alloys are of great technological value. One goal of this paper is to develop a microscopic model which predicts from *ab initio* elemental properties whether two transition metals mix to form an alloy and, if so, what is the stable atomic arrangement. The second goal is to understand the experimental trends in terms of a simple qualitative picture. To achieve these goals a model developed in a previous paper[1] (hereafter referred to as RF) and applied successfully to monovalent metals is extended to consider transition metals. First-principle calculations for atoms and elemental solids are used to construct a Hamiltonian for the alloy. The heat of formation (ΔH) is then calculated self-consistently as a function of concentration and short-range order using the alloy cluster-Bethe-lattice method.[2,3] The stable phase at zero temperature has the most negative heat of formation. Finite temperature stability is not discussed here. It can be studied by including the alloy entropy.[4,5]

Most previous calculations for the heats of formation of transition-metal alloys have been limited to specific types of atomic arrangement. First-principle band-structure calculations, such as those of Williams *et al.*,[6] could only treat ordered periodic compounds. Model calculations[7–12] were limited to either compounds or completely random alloys. The difference between the heats of formation of random and ordered configurations was generally ignored. Recently, several methods for treating a broader range of atomic arrangements have been developed. One approach[13] involves linear extrapolation from results for a completely random alloy as a function of the correlations in occupation of pairs of sites. Another approach[14] involves interpolating calculated results for ordered compounds in terms of correlations in the occupations of a few sites. The approach followed here and in RF incorporates the changes in atomic configuration directly. The effect of short-range order on ΔH is given accurately—no assumptions about linearity are required. The disadvantage of the method is that the topology of the alloy lattice is treated approximately. This may lead to errors when specific alloys are considered, but not when studying trends in alloy formation across a transition metal series.

Two different models for the mechanisms determining the heats of formation of transition-metal alloys have emerged. One is a phenomenological model developed by Miedema and co-workers[7] that builds on Pauling's work.[15] The other model[8–12] assumes that the change in the energy of the *d* bands determines ΔH and is based on simple microscopic calculations.

In Miedema's model,[7] the alloy was constructed by cutting out atoms from the pure crystals and rearranging them into an alloy. The distribution of electrons in the atoms was held fixed in this process and the energy change was assumed to be zero. Two processes were considered necessary to bring the electrons in the alloy into equilibrium. The first was charge transfer driven by an electronegativity difference $\Delta\varphi$, as in Pauling's theory.[15] The second process involved "healing" the boundary region between the two different species. The two types of atom had different electron densities $n_{\rm WS}$ at their Wigner-Seitz (WS) boundaries. Miedema argued that kinetic energy was required to smooth out the discontinuity in electron density by redistributing electrons. Thus he included a positive contribution to ΔH related to the electron density mismatch. His final result was[16]

$$\Delta H = -P(\Delta\varphi)^2 + Q(\Delta n_{\rm WS}^{1/3})^2 , \tag{1.1}$$

where P and Q were adjusted to fit available experimental values. This expression gave the correct sign for the heat of formation of a large number of alloys,[7] and quantitative agreement was reasonable when experimental values for ΔH were available. In the absence of extensive experimental data it has become a reference to which other calculations are compared.

Two points about Miedema's model are relevant to the following discussion. The first is that in transition metals the interstitial charge density $n_{\rm WS}$ is determined by the *free-electron-like s and p bands and not by the d bands.*[6,17] The *d* orbitals do not extend far from the nucleus. The

second is that Miedema adjusted values of φ and n_{WS} for individual elements to improve agreement with experiment. The adjusted values still exhibit regular chemical trends. Chelikowsky and Phillips[18] have shown that the electronegativities agree well with an orbital-radius electronegativity scale with just three adjustable parameters. Values for n_{WS} correlate with *calculated* interstitial charge densities.[6,17] However, no clear theoretical explanation for the healing contribution to ΔH has been developed. It remains uncertain whether Miedema's approach provides an accurate picture of the physical processes that determine alloy heats of formation or is merely a precise parametrization of experimental data.

Friedel[19] has shown that the cohesive energies of pure transition metals can be understood in terms of a simple model for d-band bonding. Detailed calculations[20] confirm that the free-electron-like bands contribute little to the cohesive energy. This has motivated several model calculations[8–12] for ΔH based on the changes in the d bands with alloying. Simple square band models[8–11] for the electronic density of states (DOS) based on the moments method,[21] and coherent-potential approximation[22] (CPA) calculations[12] with model DOS's have been reported. The success of these models suggests that n_{WS} is not a relevant parameter in determining the heats of formation. The same conclusion was reached by Williams *et al.*[6] based on their calculations for ordered compounds.

In this paper, the contribution of the free-electron bands to ΔH is examined explicitly for the first time. Calculations performed with and without these bands show that they do not affect the major trends in the heats of formation. This supports the view that n_{WS} is not relevant to the heat of formation of transition-metal alloys. However, the contribution of the free-electron bands does change the stable phase of several alloys and cannot be neglected in accurate calculations. Our results also provide a test of the various square band models.[8–11] Despite their success when compared to experiments, these models do not *in general* predict reliably the magnitude or sign of ΔH for the model alloys they are designed to describe. The reasons for their successes and failures are examined in Sec. IV A.

To understand the physical origin of different contributions to ΔH it is useful to develop simple pictures for the changes in the DOS with alloying. In Fig. 1(a), densities of states for two hypothetical pure metals are sketched. The bands of available valence electron levels have different widths and centers. The separated pure metals also have different Fermi levels. The simplest model for the DOS of an alloy is a superposition of the elemental DOS's [Fig. 1(b)]. The available energy levels for valence electrons on each species remain unchanged. However, charge transfers from filled electron levels on one species to lower unfilled levels on the other species to equalize the Fermi levels. The Fermi-level difference acts like an electronegativity difference:[15] ΔH is negative. In a realistic model the Coulomb potential produced by charge transfer must be included self-consistently. It acts to shift the relative positions of the centers of the elemental DOS's and limits charge transfer. However, the heat of formation in this simple *ionic bonding* model always remains negative. To understand the positive contributions to ΔH we must understand how the alloy DOS is different from a simple superposition of elemental DOS's.

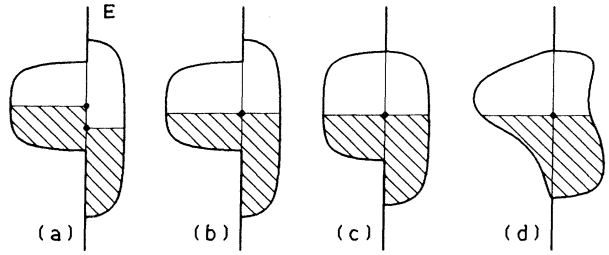

FIG. 1. Schematic partial densities of states on A (left) and B (right) atoms for separate elements (a) and the alloy (b)—(d): (b) *ionic picture,* superposition of elemental DOS's with charge transfer driven by Fermi level difference, (c) ionic picture with *band narrowing* from bandwidth disorder, (d) band deformation from state mixing, *band mixing.*

The results presented in RF and in Sec. IV indicate that the main factor favoring segregation is the difference in bandwidths of the elemental solids. This difference results in an effective narrowing of the alloy DOS that is indicated schematically in Fig. 1(c). The two species in the alloy do not bond as strongly to each other as the separate elements do, on average. The *bandwidth mismatch* contribution to ΔH is always positive.

The densities of states represented in Figs. 1(b) and 1(c) have an unphysical aspect. The two species of atom are next to each other in the alloy, and yet in certain energy regions there are electron levels on one species and not on the other. The actual alloy DOS looks like Fig. 1(d): Energy levels on the two species mix. The *band-mixing* contribution to ΔH can be either positive or negative depending on the position of the Fermi level. It is negative when the Fermi level is near the center of the band and positive when it lies near either edge of the band. The origins of this contribution to ΔH and of the bandwidth mismatch contribution are further discussed in Sec. IV A. Charge transfer is also associated with band mixing, and may be in the opposite direction from transfer driven by differences in elemental Fermi levels. A good electronegativity scale should include both contributions.

All three contributions to ΔH, ionic bonding, bandwidth mismatch, and band mixing, depend strongly on the degree of short-range order (SRO). Their relative importance varies with the constituents of the alloy. The heats of formation of monovalent metals are largely determined by the competition between ionic bonding and bandwidth mismatch.[1] In contrast, the calculations presented here show that the self-consistent contribution of ionic bonding to the heat of formation of a 4d transition-metal alloy is small. Band mixing and bandwidth mismatch of the d-electron bands are dominant in determining ΔH.

In Sec. II the short-range-order parameters and the prescriptions for determining the alloy Hamiltonian are described. The alloy cluster-Bethe-lattice method (CBLM) is described in Sec. III and extended to the case of multiorbital local bases in Appendix A. Results for all twenty-eight 4d transition-metal alloys are presented in Sec. IV and compared to experiment and previous calculations.

II. ALLOY MODEL

A. Short-range order

Experimental alloy structure determinations[23] indicate that transition-metal alloys are substitutional. Atoms are located on the sites of a periodic lattice. Only the arrangement of species on the sites is disordered. In the thermodynamic limit, the energy per site of the alloy only depends on a few macroscopic order parameters, not the specific arrangement of atoms. The local chemical environments of atoms play the dominant role in determining the energy of an arrangement.[24] The character of these environments is described by short-range-order (SRO) parameters.

The simplest macroscopic averages which measure the degree of SRO in a substitutional alloy are pair probabilities. A nearest-neighbor bond in a binary alloy of A and B atoms can have four configurations: A—A, A—B, B—A, and B—B. The fraction of bonds of type $(I$—$J)$ is denoted by $y_{IJ}(1)$. Only two independent order parameters are needed to specify $y_{IJ}(1)$ because of symmetry and normalization constraints. It is most convenient to choose these to be $x=c_A$, the concentration of A atoms, and σ, a variable describing the degree of correlation in the occupation of neighboring sites.[25] In terms of x and σ the concentrations and pair probabilities are

$$y_{IJ}(1)=c_I c_J+(2\delta_{IJ}-1)x(1-x)\sigma \ . \tag{2.1}$$

The (x,σ) parameter space is discussed in detail in RF. Three limiting types of SRO are important in the discussion that follows. For $\sigma=1$ the alloy is *segregated*, there are no A—B or B—A bonds. When $\sigma=0$ the distribution of atoms in the alloy is *random*, $y_{IJ}(1)=c_I c_J$. A *binary-ordered* arrangement is one in which either $y_{AA}(1)$ or $y_{BB}(1)$ is zero. Atoms are surrounded by unlike atoms to the maximum possible degree.

On the bcc lattice, the six next-nearest neighbors are less than 15% more distant than the nearest neighbors. The distribution of next-nearest-neighbor pairs must also be specified. In principle the next-nearest-neighbor pair probabilities $y_{IJ}(2)$ introduce a new order parameter whose value should be determined by minimizing the free energy.[4] We assume that the distribution of next-nearest neighbors is the most likely one, i.e., that it maximizes the entropy of the alloy for fixed x and σ. No exact technique for calculating the most likely next-nearest-neighbor pair probabilities on three-dimensional lattices is known.[4,5] Successive approximations based on Kikuchi's method[5] can be made, but are lattice dependent and increasingly difficult. We make the lowest-order approximation, neglecting the effect of rings of bonds as we do throughout this paper.

The probability of finding three atoms I, J, and K on sites i, j, and k joined by nearest-neighbor bonds $\{I$—$J\}$ and $\{J$—$K\}$ is approximately

$$q_{IJK}=y_{IJ}(1)y_{JK}(1)/c_J \ . \tag{2.2}$$

Corrections are needed because of correlations between the occupations of sites i and k through other paths connecting these sites. Equation (2.2) becomes exact on a Bethe lattice[26] and on the bcc lattice in the limits $\sigma=+1,0,-1$, and $x=0$ or 1. Summing (2.2) over possible occupations of j gives approximate next-nearest-neighbor pair probabilities. The resulting equations for $y_{IJ}(2)$ are identical to the equations (2.1) for $y_{IJ}(1)$ except that σ is replaced by σ^2.

B. Hamiltonian

The many-body alloy Hamiltonian is divided into three components

$$H=H_{1e}-H_{e\text{-}e}+H_{\text{ion-ion}} \ , \tag{2.3}$$

where H_{1e} is a one-electron Hamiltonian incorporating the effective potential from the ions and other valence electrons, $H_{e\text{-}e}$ is a correction for double counting the electron-electron interaction in H_{1e}, and $H_{\text{ion-ion}}$ is the ion-ion interaction. The electron coordinates are expanded in a minimal tight-binding basis of localized orthogonal orbitals centered on each atom. In terms of such a basis, the one-electron Hamiltonian is written

$$H_{1e}=\sum_{i,\mu} |i,\mu\rangle E_{i\mu}\langle i,\mu| + \sum_{i,\mu;j,\nu} |i,\mu\rangle t_{i\mu,j\nu}\langle j,\nu| \ , \tag{2.4}$$

where $|i,\mu\rangle$ is the ket for the orbital μ at site i, and $\langle i,\mu|H_{1e}|i,\nu\rangle=\delta_{\mu\nu}E_{i\mu}$.

The on-site and hopping energies, $E^0_{i\mu}$ and $t_{i\mu,j\nu}$, for ordered elements or compounds can be obtained from Slater-Koster[27] fits to first-principle band-structure calculations. Prescriptions for calculating the corresponding energies in disordered alloys where band-structure methods break down are then required. A great variety of experience[28,29] suggests that the energies are directly transferable to the alloy, provided that the volume remains constant and that there is no charge transfer.[30] Volume (Ω) controls the coupling between orbitals on different sites and hence the hopping energies. Hopping energies[31] for free-electron-like bands vary roughly as $\Omega^{-2/3}$ and for d bands as $\Omega^{-5/3}$. The on-site energies are approximately volume independent,[32] but they are affected by the Coulomb potential arising from charge transfer.

In our calculations we assume that the on-site and hopping energies depend only on the species of atom at the relevant sites and, in the case of hopping parameters, the relative positions of the sites. We take

$$\begin{aligned} t_{i\mu,j\nu}&=t_{I(i)\mu,J(j)\nu}(\vec{r}_j-\vec{r}_i) \ , \\ E_{i\mu}&=E^0_{I(i)\mu}+\overline{\Phi}_{I(i)\mu} \ , \end{aligned} \tag{2.5}$$

where $I(i)$ denotes the species at site i, $t_{I\mu,J\nu}(\vec{r})$ and $E^0_{I\mu}$ are intrinsic tight-binding parameters, and $\overline{\Phi}_{I(i)\mu}$ is the mean effective Coulomb potential seen by the μ orbital on a type-I atom in a given alloy. In principle the on-site and hopping energies may depend on the particular distribution of species around a given site or bond. However, the heat of formation depends mainly on the mean values of these energies rather than on their fluctuations which should in any event be small. The calculation of $\overline{\Phi}_{I\mu}$, $H_{\text{ion-ion}}$, and $H_{e\text{-}e}$ from the charge transfers is described in detail in the next section.

Volume dependence of the hopping energies is not in-

TABLE I. Intersite tight-binding parameters (eV) for Nb and Mo (calculated from the results of Ref. 43).

	Nb	Mo		Nb	Mo
$(dd\sigma)_1$	−1.25	−1.30	$(ss\sigma)_1$	−1.02	−1.10
$(dd\pi)_1$	+0.63	+0.62	$(ss\sigma)_2$	−0.64	−0.71
$(dd\delta)_1$	−0.02	+0.01	$(ss\sigma)_3$	−0.04	−0.03
$(dd\sigma)_2$	−0.77	−0.78	$(sd\sigma)_1$	−1.41	−1.46
$(dd\pi)_2$	−0.02	−0.06	$(sd\sigma)_2$	−0.67	−0.75
$(dd\delta)_2$	+0.05	+0.06	$(sd\sigma)_3$	−0.07	−0.07
$(dd\sigma)_3$	+0.09	+0.11			

cluded. The justification for this is that as a group binary alloys obey Végard's law[33] quite well:[34] Each atom maintains its intrinsic volume in the alloy. Any deviations from Végard's law tend to be correlated with the heat of formation:[35] Strongly bound alloys ($\Delta H \ll 0$) contract and alloys with segregating tendencies ($\Delta H \gg 0$) expand. The resulting changes in bandwidth act to reinforce the ordering or segregating tendencies. Thus calculations that assume hopping parameters are directly transferable to the alloy should predict the correct sign for ΔH though not necessarily the exact magnitude. Errors are smallest in a family of alloys like the 4*d* transition-metal alloys where the constituent elements have similar volumes. Results for the monovalent metal alloys where size differences are much larger were in good agreement with experiment.[1]

The intrinsic tight-binding parameters $E^0_{I\mu}$ and $t_{I\mu,J\nu}(\vec{r})$ are determined from first-principle atomic and band-structure calculations as described in Sec. II D. Calculations for pure metals are plentiful and are used to determine $t_{I\mu,I\nu}(\vec{r})$. Ordered alloy calculations are less common and are harder to fit unambiguously. Therefore, to obtain $t_{A\mu,B\nu}(\vec{r})$, we use the convention

$$t_{A\mu,B\nu}(\vec{r})=[t_{A\mu,A\mu}(\vec{r})t_{B\nu,B\nu}(\vec{r})]^{1/2} . \tag{2.6}$$

This relation can be derived from Hückel-type,[36] free-electron[37] or Korringa-Kohn-Rostoker arguments. Deviations from this rule arise if the two species are very different in size. However, Eq. (2.6) remains an upper bound. As discussed in RF this relation is physically important and is responsible for the bandwidth-mismatch contribution to ΔH.

C. Charge transfer

The concentration, SRO, and one-electron Hamiltonian determine the average local DOS for each orbital of each species and thence the mean charge transfers. The resulting Coulomb potential must be included self-consistently in the one-electron Hamiltonian. The total Coulomb potential $\Phi_{I\mu}$ is calculated in two parts: An intrasite contribution $\psi_{I\mu}$, and an intersite contribution Ψ_I, which is the same for all orbitals.

In RF it was shown that the intersite contribution to the Coulomb potential cannot be calculated in a local approximation[3,38] because of the long-range nature of the Coulomb interaction. A scheme for summing the contributions to Ψ_I from arbitrarily distant sites on the true alloy lattice was presented. Each I atom was assigned the mean[39] electron transfer Δn_I. An approximate pair correlation function was derived which gave the probability of finding either species at a given distance from an I atom. This correlation function is exact in the random and segregated limits for all concentrations and for the binary-ordered stoichiometric AB compound. It is consistent with the next-nearest-neighbor pair probabilities that were obtained in Sec. II A. The result for the intersite contribution to the Coulomb potential was

$$\Psi_I = V\alpha(\sigma)\Delta n_I , \tag{2.7}$$

where V is the nearest-neighbor Coulomb interaction between unit charge transfers, and $\alpha(\sigma)$ is an effective Madelung sum with no concentration dependence. For the bcc lattice $\alpha(\sigma)$ is given approximately by[1]

$$\alpha(\sigma)=8.245\sigma/(1-\sigma)^2-0.245\sigma+0.055\sigma^2 . \tag{2.8}$$

The intrasite contribution to the Coulomb potential has been widely discussed in the context of elemental systems,[40] and included in some CPA calculations.[12] In the Hartree-Fock approximation with no spin ordering, the intrasite Coulomb potential is[12]

$$\psi_{I\mu}=\sum_{\nu}\tfrac{1}{2}U_{I\mu\nu}\Delta n_{I\nu}+\sum_{\nu(\neq\mu)}\tfrac{1}{2}(U_{I\mu\nu}-J_{I\mu\nu})\Delta n_{I\nu} , \tag{2.9}$$

where $U_{I\mu\nu}$ and $J_{I\mu\nu}$ are the direct and exchange interactions, $\frac{1}{2}\Delta n_{I\nu}$ is the change relative to the pure material in the number of electrons per spin in orbital ν, and the first and second terms come from opposite and like spin electrons, respectively. In the most general case considered here μ and ν represent s or d orbitals.

Several calculations of direct and exchange interactions have been reported.[40] The exchange integrals between all d orbitals on an I atom are found to be approximately equal: $J_{I\mu\nu}=J_{Idd}$. The direct integral of an orbital with itself, U_{Idd}, is larger than the direct integrals between different orbitals, which are all approximately equal to U'_{Idd}. If $\frac{1}{2}U_{Idd}=U'_{Idd}-\frac{1}{2}J_{Idd}$ the on-site shifts of all d orbitals will be equal regardless of the distribution of charge transfer among them.[41] Calculated values satisfy this relation.[40] Thus Eq. (2.9) can be written as

$$\begin{aligned}\psi_{Is}&=u_{Iss}\Delta n_{Is}+u_{Isd}\Delta n_{Id} ,\\ \psi_{Id}&=u_{Isd}\Delta n_{Is}+u_{Idd}\Delta n_{Id} ,\end{aligned} \tag{2.10}$$

where Δn_{Id} is the total charge transfer to the manifold of

TABLE II. Bandwidths of d and s bands.

Element	$\Omega_{\text{expt.}}$[a] (Å^3/atom)	W_d calc.[b] (eV)	$\left[\frac{\Omega_{\text{calc.}}}{\Omega_{\text{expt.}}}\right]^{5/3}$	W_d scaled (eV)	W_g (eV)
Y	33.11	7.0	0.88	6.2	8.9
Zr	23.31	8.6	0.89	7.7	11.2
Nb	17.99	9.1	0.99	9.0	13.8
Mo	15.58	9.0	1.03	9.3	15.2
Tc	14.20	8.4	1.08	9.1	15.3
Ru	13.59	7.4	1.11	8.2	16.0
Rh	13.77	6.3	1.10	6.9	15.6
Pd	14.71	4.9	1.08	5.3	14.9

[a]C. Kittel, *Introduction to Solid State Physics*, 5th ed. (Wiley, New York, 1976), pp. 31–32.
[b]Reference 46.

d states and

$$u_{Iss}=U_{Iss}/2\ ,\quad u_{Isd}=(U_{Isd}-J_{Isd}/2)\ ,\quad u_{Idd}=(U'_{Idd}-J_{Idd}/2)\ . \tag{2.11}$$

If correlation is properly included the u_I have different values. They are treated here as phenomenological parameters incorporating the effect of the exact electron-electron interaction for small charge transfers.

The electron-electron and ion-ion interactions, normalized to the number of atoms, are given by

$$H_{e\text{-}e}=\tfrac{1}{2}\sum_I c_I \sum_{\beta\gamma} u_{I\beta\gamma} n_{I\beta} n_{I\gamma}+\frac{e^2}{N}\sum_{ij}\frac{n_i n_j}{2\epsilon r_{ij}}\ ,$$
$$H_{\text{ion-ion}}=\frac{e^2}{N}\sum_{ij}\frac{Z_i Z_j}{2\epsilon r_{ij}}\ , \tag{2.12}$$

where $-|e|n_i$ and $|e|Z_i$ are the total valence and ionic charges, β and γ stand for s or d orbitals, and r_{ij} is the distance between sites i and j. The net contribution of these terms to the total energy largely cancels because $n_i=Z_i+\Delta n_i$:

$$H_{\text{ion-ion}}-H_{e\text{-}e}=-(1/N)\sum_i (Z_i+\tfrac{1}{2}\Delta n_i)\sum_j \frac{e^2\Delta n_j}{\epsilon r_{ij}} -\tfrac{1}{2}\sum_I \sum_{\beta\gamma} c_I u_{I\beta\gamma} n_{I\beta} n_{I\gamma}\ . \tag{2.13}$$

Recognizing the sum over j in the first term as the interatomic Coulomb potential at site i and replacing it by its mean for each species gives

$$H_{\text{ion-ion}}-H_{e\text{-}e}=-V\alpha(\sigma)\sum_I c_I(n_I-\tfrac{1}{2}\Delta n_I)\Delta n_I -\tfrac{1}{2}\sum_I \sum_{\beta\gamma} c_I u_{\beta\gamma} n_{I\beta} n_{I\gamma}\ . \tag{2.14}$$

D. Elemental tight-binding parameters

The band structures of elemental 4d transition metals in the bcc structure were modeled with a free-electron-like s band and five d bands. The d band structures of transition metals are very similar.[17,28,42] Andersen[42] has shown that they are well described by "canonical bands." For elements in a given crystal structure, only the overall bandwidth and the on-site energy depend on the atomic species.

Pickett and Allen[43] have made detailed Slater-Koster[27] tight-binding fits to augmented plane-wave band-structure calculations[44,45] for bcc Nb and Mo. Their results are summarized in Table I. Slater and Koster's notation is followed. Matrix elements are denoted by the type of orbital on each site, s or d, and the magnitude of the orbitals' angular momenta m about the axis connecting the sites: σ, π, and δ correspond to $|m|=0$, 1, and 2, respectively. Matrix elements between nth nearest neighbors have subscript n.

Table I shows clearly that second-nearest-neighbor hopping on the bcc lattice is important, and that third-nearest-neighbor hopping is negligible. The matrix elements $(dd\delta)_1$, $(dd\pi)_2$, and $(dd\delta)_2$ are also very small and may be set to zero. The ratios among the remaining parameters are nearly equal in Nb and Mo:

$$\frac{(dd\pi)_1}{(dd\sigma)_1}=-0.49\pm0.01\ ,\quad \frac{(dd\sigma)_2}{(dd\sigma)_1}=0.61\pm0.01\ . \tag{2.15}$$

Following the ideas of Andersen[42] and Harrison[28] these ratios were assumed to be constant for all 4d transition metals. Values for $(dd\sigma)_1$ for each element were calculated by scaling the value for niobium by the ratio of elemental d-band widths.

Moruzzi *et al.*[46] have calculated first-principle band structures for all 4d transition metals in the bcc structure. Table II lists their results for d-band widths at the calculated equilibrium volume. As discussed in Sec. II B, the d-band width is highly volume dependent. Errors in the calculated volume produce larger errors in d-band width. These errors would affect ΔH by changing the amount of bandwidth mismatch. To prevent this, the calculated bandwidths were scaled (Table II) to the experimental volume using the relation $W_d\propto\Omega^{-5/3}$ mentioned in Sec. II B. The *scaled* bandwidths agree well with the results of less sophisticated methods that were calculated at the ex-

perimental volume.[42,47,48] The scaled bcc bandwidths were used in the calculations reported in Sec. IV.

The s and p bands of transition metals are essentially free-electron-like. In the calculations presented here, they were modeled by a single s band with a free-electron bandwidth[49]

$$W_s=\frac{3\pi^2\hbar^2}{2ma^2}\ , \tag{2.16}$$

where a is the nearest-neighbor separation and m is the free-electron mass. Values for W_s are given in the last column of Table II. Equation (2.16) is obtained by finding the energy difference between free-electron levels at the zone center Γ and corner H of the bcc Brillouin zone.

For each element, $(ss\sigma)_1$ was scaled so that the cluster-Bethe-lattice method (CBLM) gave the correct bandwidth W_s. The ratio $(ss\sigma)_2/(ss\sigma)_1$ was held fixed at its value in Nb and Mo where (Table I)

$$\frac{(ss\sigma)_2}{(ss\sigma)_1}=0.64\pm0.01\ . \tag{2.17}$$

These prescriptions reproduce the values for $(ss\sigma)_1$ in Nb and Mo within 10% and the ratio between values in the two materials to 2%.

The s-d hybridization terms in Nb and Mo are proportional to the geometric mean of $(ss\sigma)_1$ and $(dd\sigma)_1$ as suggested by Harrison's equations.[28] The proportionality constants were calculated from Table I

$$\begin{aligned}\frac{(sd\sigma)_1}{[(ss\sigma)_1(dd\sigma)_1]^{1/2}}&=1.24\pm0.02\ ,\\ \frac{(sd\sigma)_2}{(sd\sigma)_1}&=0.49\pm0.02\ .\end{aligned} \tag{2.18}$$

The choice of on-site energies has been the focus of debate. Pettifor[9] argued that the eigenvalue for the appropriate atomic configuration should be used for the d-band center. Harrison has successfully used atomic eigenvalues in calculations for compounds of transition metals and non-transition-metals.[28] However, Varma[10] has argued that the d-band centers should reflect the change from atomic boundary conditions when the solid is formed. Thus he used eigenvalues calculated with the renormalized atom method[50] in his treatment of transition-metal alloys. The correct choice of elemental on-site energies depends on one's model for the charge distribution in the alloy before charge transfer occurs. The arguments below explain why free-atom eigenvalues are more appropriate for tight-binding calculations such as those reported here. In Sec. IV we note that ΔH is relatively insensitive to the on-site energies. However, calculations using renormalized atom eigenvalues[51] do not agree as well with experiment and band-structure calculations[6,46] as the calculations using free-atom eigenvalues reported in Sec. IV.

The renormalized atom method[50] was designed to calculate properties of solids from an atomic picture. The atomic charge was confined to a Wigner-Seitz sphere with volume equal to that occupied by each atom in the solid. Wave functions were obtained by truncating free-atom wave functions at the sphere boundary and scaling them to maintain normalization. The Hartree potential increased as the volume decreased. For 4d transition metals, the d eigenvalues of renormalized atoms were about 7 eV higher than free-atom eigenvalues. The magnitude of the eigenvalue shift varied with equilibrium volume across the 4d series. The separation between renormalized atom d eigenvalues on different species changed in sign and magnitude ($\sim$2 eV) from the separation between free-atom eigenvalues. The renormalized atom method has successfully reproduced cohesive energies[47] and bandwidths of elemental transition metals. However, neither of these quantities depends on the absolute value of the on-site energy.

In a renormalized atom picture the alloy is constructed by combining neutral Wigner-Seitz spheres of the constituent species. This is also the initial charge density in the self-consistent calculations of Williams and coworkers.[6,46] Their calculations give on-site energy differences before charge transfer which are close to the differences in renormalized atom eigenvalues. However, this initial charge density is discontinuous at the Wigner-Seitz boundaries.[6] It is not compatible with the tight-binding picture on which our calculations are based.

The non-self-consistent charge density in a tight-binding alloy calculation should correspond to a superposition of atomiclike charge densities obtained by occupying the tight-binding orbitals on each species to the same extent as in the pure elements. The tight-binding orbitals are not truncated at the Wigner-Seitz sphere as the renormalized atom wave functions are. Thus the resulting charge density is continuous. The difference between renormalized atom and tight-binding charge densities consists of a dipole layer at the Wigner-Seitz boundary. The associated potential step produces a shift in the on-site energy differences given by the two models.

To justify the choice of atomic on-site energies for our calculations we begin from the observation that the charge density in elemental transition metals is close to a superposition of atomic charge densities.[28,29,52] The non-self-consistent Hartree potential for an alloy is thus close to a superposition of atomic Hartree potentials. The attractive potential from neighboring sites lowers the on-site energy relative to the atomic eigenvalue and orthogonalization to orbitals on neighboring sites raises the on-site energy. The shifts tend to cancel. In addition, in a random alloy the shifts on both species are approximately equal because they see the same environment. The difference in on-site energies *in the alloy* is thus close to the difference in atomic eigenvalues. The difference in the on-site energies of *separate pure elements* is ambiguous because of surface contributions and does not affect the heat of formation. It may be related to the difference in renormalized atom eigenvalues.

Calculated atomic potentials were superposed in an effort to understand the origin of the eigenvalue shifts given by the renormalized atom method. The Hartree potential in the region near the Wigner-Seitz boundary was negative and strongly volume and species dependent. In the renormalized atom method the Hartree potential in this region was always set to zero. The difference between renormal-

TABLE III. Calculated free-atom eigenvalues (eV).

Element	s	d
Y	−3.60	−1.88
Zr	−3.80	−2.65
Nb	−3.94	−3.41
Mo	−4.03	−4.17
Tc	−4.11	−4.94
Ru	−4.17	−5.72
Rh	−4.22	−6.51
Pd	−4.26	−7.31

ized atom and free-atom eigenvalues correlated well with our calculated potential at the Wigner-Seitz boundary.

For the reasons detailed above, atomic eigenvalues were used for the elemental on-site energies in the calculations reported here. The eigenvalues, listed in Table III, were calculated for an atom with one s electron and all d orbitals equally occupied. Exchange and correlation were included using the local-density functional calculated by Ceperley and Alder.[53] Relativistic effects were small and were not included.[54] Crystal-field splitting was also not included. The metals are not magnetic and thus the atomic eigenvalues listed do not include spin polarization.

CBLM results for the pure elements with these on-site energies and the hopping parameters described above provide a reasonable description of the elemental DOS's. The separations between the d-band centers and the bottoms of the s bands are in good agreement with band-structure results. The calculated s occupancies are about one electron in keeping with the assumptions made in calculating the on-site energies.[55]

The only remaining elemental parameters are the Coulomb energies. In their CPA calculations, Gautier *et al.*[12] have estimated[56] that $u_{dd} \approx 1.6$ eV. Williams *et al.*[6] have calculated s and d charge transfers and the changes in d-band on-site energies with self-consistency in ordered $4d$ transition-metal compounds with the CsCl structure. Their results are consistent with

$$\begin{aligned} u_{sd} + V\alpha(-1) &= 0.4 \ , \\ u_{dd} + V\alpha(-1) &= 1.4 \ , \end{aligned} \tag{2.19}$$

measured in eV. A reasonable value of $V = 0.3$ eV does not lead to charge-density wave instabilities[1] if $u_{ss} > 0.5$ eV. The values used in most calculations were (in eV)

$$u_{ss} = 0.7 \ , \quad u_{sd} = 0.9 \ , \quad u_{dd} = 1.9 \ , \quad V = 0.3 \ . \tag{2.20}$$

The above Coulomb energies are substantially smaller than the unscreened values for free atoms. Calculations[57] for Mo *atoms* gave (in eV)

$$u_{ss} = 5.3 \ , \quad u_{sd} = 6.1 \ , \quad u_{dd} = 7.9 \ , \quad V = 3.0 \ , \tag{2.21}$$

where V was calculated using the equilibrium lattice constant and vacuum dielectric constant. As discussed in RF, screened values of u_I are appropriate in minimal basis tight-binding calculations because screening by core orbitals and high-energy valence electrons changes the effective dielectric constant ϵ from the vacuum value ϵ_0. In the self-consistent *ab initio* band-structure calculations[6] from which (2.19) was obtained, the decrease in the u_I is related to changes in the nature of the s and d orbitals. Higher valence levels are mixed in when the local environment changes through alloying.

III. ALLOY CLUSTER-BETHE-LATTICE METHOD

The alloy CBLM is an approximate technique[2,3] for calculating the configuration averaged local density of states (LDOS) of an alloy at arbitrary x and σ. A self-consistent mean-field approximation is made which is very much in the spirit of Bethe's original approximation for magnetic systems.[58] A small cluster of atoms is treated exactly and the remainder of the alloy is replaced by an effective field, in this case a self-energy. Two approximations are made. (1) The form of the effective field (site-diagonal) is only exact on a lattice with the same coordination number as the real lattice, but with no rings of bonds. Such lattices have been named Bethe lattices after the approximation.[26] (2) The value of the effective field is calculated self-consistently in a mean-field approximation, incorporating the mean distribution of neighbors as given by the pair probabilities.

The alloy CBLM models the mean local environment of all atoms in the alloy very well. The coordination number and mean distribution of nearest neighbors are reproduced exactly. The effect of the first approximation is to simplify the topology of the alloy outside the cluster. It is replaced by Bethe lattices with the same coordination number, Hamiltonian matrix elements, and SRO. On this approximate topology, the mean-field approximation provides accurate values for the total energy as a function of SRO and disorder in the Hamiltonian (diagonal, off-diagonal, and environmental).[51] Fluctuations in local environment affect some alloy properties,[59] but not the total energy.[12]

In this paper we present results for a simple single-atom cluster. Neglect of topological effects is justified by the following considerations.

(1) Only *changes* in *integral quantities,* total energy, and charge, are considered. Absolute errors cancel and exact theorems[60] place limits on errors in integrated quantities. The largest errors will occur when the Fermi level lies near a strong structure in the alloy DOS which is not reproduced by the alloy CBLM.

(2) Calculations for the heats of formation of random alloys with the CPA based on either fcc- or bcc-like bands and calculations with the alloy CBLM all give similar results as long as the elemental bandwidths are the same.[12,51]

(3) Previous calculations for monovalent metals were in good agreement with experimental data.[1]

(4) No technique developed to date can include SRO nonperturbatively[13,14] on any lattice other than a Bethe lattice. This is related to the fact that higher-order cluster probabilities are needed to define the configuration probabilities on other lattices.[61]

Previous derivations and applications[2,3,38] of the alloy

CBLM have been limited to the case of a single s-like orbital per site. For the calculation presented here the method was extended to include five d orbitals and one s orbital on each site. Both nearest- and next-nearest-neighbor hopping are important on the bcc lattice (Sec. II D) and were included. The six next-nearest neighbors were incorporated in the Bethe lattices as nearest neighbors of a different type. Numerical evaluation of the DOS and total energy is greatly facilitated through the use of group theory and by deforming the contour of integration into the complex plane. These techniques are described in Appendix A.

IV. RESULTS FOR 4d TRANSITION METALS

A. Comparison to previous microscopic models

A variety of different approximations were made in previous microscopic model calculations[8–12] for ΔH that are not made in our calculations. None of these models included the effect of s electrons or SRO. Self-consistency was only considered explicitly in CPA calculations.[12] These three factors are discussed below in separate sections. The simple square band models for the alloy DOS suggested by Cyrot and Cyrot-Lackmann[8] and RF, and by Pettifor[9] and Varma,[10] are examined briefly here. These models provide approximate solutions for the DOS and heat of formation of well-defined model alloys. No dependence on lattice type is included. Results from the alloy CBLM and CPA for the same model alloys in the random configuration on a Bethe lattice have been calculated to test the square band models.[51] The alloy CBLM and CPA heats of formation agree to about $10^{-4}W$ where W is the bandwidth of the alloy. The various square band models give a wide spread of values for ΔH which do not *in general* agree in magnitude or sign with the CPA and CBLM results. However, each of the square band models is reasonably accurate *for specific alloy systems.* The reasons for this are discussed below. The discussion helps to clarify the origin of the contributions to ΔH that are illustrated in Fig. 1.

All of the simple square band models are based on the moments method.[21] The first few moments

$$\mu^n \equiv \int E^n D(E) dE \ , \tag{4.1}$$

of the DOS, $D(E)$, in a random alloy are easily calculated. The centers and widths of square bands are fitted to these moments to model the alloy DOS. The models mentioned above all fit the first three moments of the DOS (μ^0, μ^1, and μ^2) and, in the case of RF, μ^3. However, the DOS's that are generated are very different. The models proposed by Cyrot and Cyrot-Lackmann[8] and RF are ionic models. Separate square bands for the local DOS on each species are constructed. The effects of ionic bonding and bandwidth mismatch [Figs. 1(b) and 1(c)] are incorporated accurately, but band mixing [Fig. 1(d)] is not. The model proposed by Pettifor[9] and Varma[10] is a band-mixing model. A single square band is constructed for the *total* DOS. The band-mixing contribution to ΔH is reproduced quite well. Bandwidth mismatch is included also, but not as accurately.

These two types of model lead to different heats of formation. For monovalent metals, the ionic model gives values for ΔH that are in good qualitative agreement with alloy CBLM results for the random configuration.[1,51] The band-mixing model gives unphysical results—the random alloy is always stable. Pettifor initially applied his band-mixing model to the case of equal Fermi levels and bandwidths.[9] For such alloys band mixing provides the *only* contribution to ΔH. The ionic model gives $\Delta H = 0$, while the band-mixing model gives values for ΔH that are in good agreement with the alloy CBLM and CPA.

The conclusion to be drawn from these results is that the square band models only give reliable results for the heats of formation of the model alloys they attempt to describe when at least one of the contributions to ΔH illustrated in Fig. 1 is small. Conversely when one of the square band models works it implies which contributions to ΔH are important. The reason that the models are not successful for general alloys is that the first three moments of the DOS do *not* provide sufficient information about the changes in the DOS with alloying. In fact, neglecting changes in on-site energy difference due to self-consistency, these moments are *exactly the same* in the segregated and random configurations in the case of zero bandwidth mismatch. The lowest-order moment which is not the same in the two configurations is μ^4. The difference is *lattice independent* and is reproduced exactly by the alloy CBLM with single atom cluster.[51]

The behavior of the band-mixing contribution to ΔH, which is important in transition-metal alloys, can be understood from the above statements. For the case of zero bandwidth disorder, the segregated and random configuration DOS's have the same center, μ^1, and second moment, μ^2, but their band edges are different.[62] As illustrated in Fig. 1 the segregated DOS extends over a greater energy range than the random DOS. To maintain the same second moment, the random DOS must have more spectral weight near its band edges. If the bands are nearly empty or full the segregated phase has a lower energy because of the states at extremely low energies. If the bands are half-full the random phase has a lower energy because of the shift in spectral weight towards the band edges. These changes in sign of ΔH with band filling follow from exact theorems based on the number of identical moments.[21,60] When bandwidth disorder is introduced, the second moment of the DOS of the random alloy becomes lower than that of the segregated configuration. The random DOS is spread over a smaller energy range and ΔH increases. The physical picture for this contribution is that the coupling between unlike species is weaker than the average coupling between like species [Eq. (2.6)].

The most interesting result suggested by the various square band models is Pettifor's[9] simple expression for ΔH in terms of the mean, $\bar{N}$, and difference, ΔN, in the number of valence d electrons in the constituent elements. Based on the band-mixing square band model, the linear variation of atomic eigenvalues across the 4d series and a quadratic variation in elemental solid volumes, Pettifor found

$$\Delta H = (\Delta N)^2 \overline{\Delta H}(\bar{N}) \ . \tag{4.2}$$

for $x = \frac{1}{2}$. There are several difficulties with Pettifor's

evaluation of $\overline{\Delta H}$. However, for 4*d* transition-metal alloys this relation is roughly obeyed by Miedema's[7] results and the results of Williams *et al.*[6] Williams *et al.* point out that it can be thought of as a Taylor series expansion in small ΔN, however it holds fairly well for $\Delta N = 7$. Non-self-consistent results with the alloy CBLM do not necessarily obey this relation. However, our *self-consistent* results do follow this behavior. All our results show a strong dependence on SRO as discussed below, i.e.,

$$\Delta H = (\Delta N)^2 \overline{\Delta H}(\overline{N},\sigma) \; . \tag{4.3}$$

for $x = \frac{1}{2}$. The reasons for these findings are discussed in subsequent sections. Relation (4.3) is useful because it allows us to illustrate the behavior of the heats of formation of all twenty-eight 4*d* transition-metal alloys while plotting only results for alloys with $\Delta N = 1$.

B. The role of *s* electrons

The *s* electrons affect ΔH in several different ways. There are direct contributions to ΔH from ionic bonding, bandwidth mismatch, and band mixing of *s* bands. The *s* electrons also contribute to ΔH through the *d* bands by changing the number of *d* electrons, screening *d* charge transfer, and altering the *d*-band shape via *s-d* hybridization. Each of these contributions can be examined independently with the alloy CBLM.

Calculations were performed for *d* bands only, and for *s* and *d* bands with and without *s-d* hybridization. For calculations including *d* bands only, the number of *d* electrons in the pure elements was set equal to the value calculated for *s* and *d* bands with hybridization. Self-consistent results for the heat of formation of the random configuration of alloys with $\Delta N = 1$ and $x = \frac{1}{2}$ are plotted in Fig. 2. Screened Coulomb integrals and the bandwidths and centers described in Sec. II D were used. Results calculated non-self-consistently, results for the binary-ordered configuration, and results for other elemental tight-binding energies show the same features. The energies calculated for *d* bands only and for *s* and *d* bands without hybridization are almost identical. Including *s-d* hybridization does not change the parabolic trend of ΔH across the 4*d* series. However, it does change the sign of the random and/or binary-ordered energies of several of the twenty-eight 4*d* alloys. This has important consequences for their phase diagrams. The free-electron bands cannot be ignored in accurate calculations.

The results shown in Fig. 2 are easily understood. The independent contribution of *s* electrons to ΔH is small because the *s* bands of all elements have similar centers, widths, and band fillings, and because there are many more *d* electrons. Charge transfer of *s* electrons, which changes the total *d*-electron occupation or screens *d*-electron charge transfer, is small because the *s*-band DOS is much smaller than the *d*-band DOS (1:7). Also, the *d-d* Coulomb repulsion is strongest, so that *d* electrons screen *d* charge transfer most effectively. Hybridization of *s* and *d* bands is important because it changes the *d*-band DOS *over the entire bandwidth.* The *d* band is effectively broadened by hybridization with the wider *s* band. Increasing the *d*-band width lowers the magnitude of bonding (negative) contributions to ΔH which depend on the ratio of the on-site energy difference to the bandwidth. The positive contribution to ΔH from bandwidth mismatch *increases* at the same time. The result is an increase in ΔH for all alloys. Only heats of formation for alloys with $\Delta N = 1$ are shown in Fig. 2. The positive contribution to ΔH from *s-d* hybridization increases as $(\Delta N)^2$ [see (4.3)] and thus remains significant for all alloys.

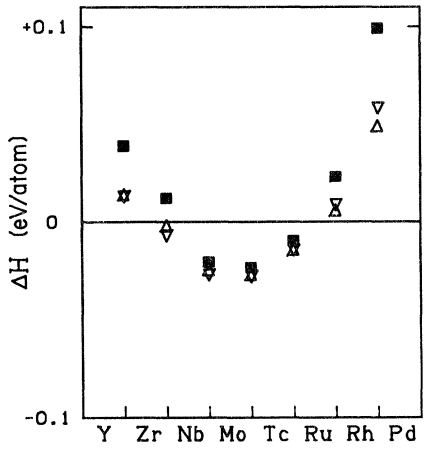

FIG. 2. Heats of formation for random equiconcentration alloys of neighboring elements in the Periodic Table calculated with free atomic on-site energies and screened Coulomb interactions for *d* bands only (down pointing triangles); *s* and *d* bands without *s-d* hybridization (up pointing triangles) and with *s-d* hybridization (solid squares).

The results just described indicate that *s* electrons do not play the strong role in screening *d* charge transfer that was assumed in Varma's model.[10] Varma argued that conduction electrons transferred so as to minimize the energy of the *d* bands. Rather than considering charge transfer explicitly, he treated the *d*-band centers as variational parameters. It is evident from Fig. 2 that this model is not appropriate. The presence of *s* electrons *does not* allow optimization of the *d* electron binding. This is not an artifact associated with the use of screened *u*'s. Heats of formation calculated with unscreened *u*'s show the same behavior. Values for ΔH in all three cases illustrated in Fig. 2 are shifted in a positive direction. The magnitude of the shift is relatively uniform and small—about the size of the plotting symbols in Fig. 2.

The similarity in the values for ΔH with screened and unscreened *u*'s is surprising. The two sets of Coulomb energies differ by a factor of 5. In an ionic bonding model, ΔH would change substantially. The effect of self-consistency is discussed in the next section.

C. Self-consistency

Non-self-consistent results for the heats of formation of transition-metal alloys depend strongly on the difference in elemental on-site energies. In contrast, all self-consistent results show the same *qualitative* behavior: heats of formation vary parabolically across the transition-metal series and obey relation (4.3) approxi-

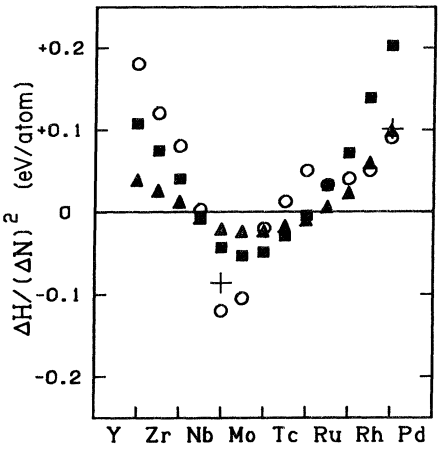

FIG. 3. Alloy CBLM results for $\Delta H/(\Delta N)^2$ at $x=\frac{1}{2}$ in the random (solid triangles) and binary-ordered (solid squares) configurations of 4*d* alloys with $\Delta N \leq 2$. Also shown are band-structure results from Ref. 46 for the heats of formation of compounds in the CsCl structure (open circles), and measured random heats of formation (crosses).

mately. As noted above, the heats of formation are fairly insensitive to the magnitude of the Coulomb interaction energies. These results indicate that the self-consistent contribution from ionic bonding to the heats of formation of transition metals is small. The band-mixing contribution to ΔH remains large after self-consistency is reached because the difference in *d*-band filling leads to differences in the *d*-band centers. This *did not happen* in monovalent metals[1] where the band filling was constant. The bandwidth mismatch contribution is also unaffected by self-consistency. The band mixing and bandwidth mismatch contributions both obey relation (4.3). (In the case of bandwidth mismatch this follows from the parabolic trend in bandwidths across the 4*d* series.)

The success of Pettifor's[9] model is understood from these results. His choice of input parameters eliminates the ionic bonding contribution to ΔH. This is precisely the effect that self-consistency has in more detailed calculations. The band-mixing energy remains important and is given fairly accurately by his square band model. The difficulty with Pettifor's model is in his picture for the positive contribution to ΔH. He attributes it explicitly to differences in elemental volume rather than differences in elemental bandwidths. This shifts the minimum of $\overline{\Delta H}$ away from $\overline{N}=5$ (see Fig. 1 of Ref. 9) and increases $\overline{\Delta H}$ in magnitude relative to the correct value. The physical picture Pettifor proposes of atoms reaching equal volumes in the alloy does not explain why Végard's law[33] holds and is contradicted by first-principle calculations[46] which show that each species tends to maintain its intrinsic volume. The bandwidth mismatch model used here is more physical and yields more accurate values for ΔH as shown below.

D. Dependence of ΔH on SRO

In earlier work[6,7,9–11] the difference between the heats of formation of random and binary-ordered configurations has not been appreciated. Calculated energies for the random configuration[9–11] and for ordered compounds[6,7] have been compared directly to each other and to experimental values for different configurations. This is the first microscopic calculation to consider explicitly the variation of the heat of formation with SRO in the 4*d* transition-metal alloys. As shown in Fig. 3, the dependence of ΔH on SRO is strong.

Figure 3 compares self-consistent alloy CBLM results for $\Delta H/(\Delta N)^2$ in the random and binary-ordered configurations at $x=\frac{1}{2}$. Screened Coulomb interactions were used. Results for alloys with $\Delta N=1$ and 2 are plotted to show that relation (4.3) is approximately obeyed. Values of $\Delta H/(\Delta N)^2$ calculated for alloys with larger ΔN fall close to these results but are slightly smaller in magnitude. The random and binary-ordered heats of formation both vary parabolically across the series. However, the magnitude of the binary-ordered energy is larger. The band-mixing and bandwidth mismatch contributions to ΔH are largest in magnitude for the binary-ordered configuration where no like-atom nearest-neighbor bonds remain.

A simple trend in the stable phase is found. The segregated configuration is stable for large and small values of $\overline{N}$. For these alloys, bandwidth mismatch is large (Table II) and the band-mixing energy is more positive. The binary-ordered phase is stable for $\overline{N}$ near 5. In these alloys bandwidth mismatch is small and the band-mixing energy is large in magnitude and negative. The energy of the random configuration is only lowest in the crossover region where all heats of formation are small. Note that Fig. 3 only gives values for ΔH at $x=\frac{1}{2}$. In most cases when all other concentrations are considered the random configuration does not have the lowest heat of formation.

Williams and co-workers[6,46] have performed *ab initio* calculations for the heats of formation of all 4*d* transition-metal alloys in the CsCl structure relative to elements in the bcc structure. Their results for alloys with $\Delta N=1$ and 2 are also plotted in Fig. 3. Agreement with our binary-ordered results for $\Delta N=1$ and 2 is fair. Values from the two methods for alloys where $\Delta N>2$ are in much better agreement. For $\Delta N=5$, 6, and 7 *the plotted points overlap.* The discrepancy for $\Delta N=1$ and 2 is understood as a band-shape effect. There is a strong pseudogap in the *d*-band DOS of transition metals in the bcc structure. The Fermi level lies in this gap for band fillings between those of Nb and Mo, and it is believed to be important in stabilizing the bcc phase of these elements. This gap is not reproduced by the alloy CBLM with single-atom cluster. Experiment and theory[43] suggest that the pseudogap remains in Nb-Mo alloys. It should give a strong rigid band[63] contribution to ΔH. As ΔN increases the on-site energy difference becomes increasingly larger than the width of the pseudogap and its importance to ΔH decreases. This contribution to ΔH does not obey relation (4.3).

The band-shape effect described above clearly depends on the specific crystal structures of the elements and alloy. Williams *et al.*[46] have also calculated the heats of formation of compounds in the CuAu structure from elements in the fcc structure. Their results show the same trends with $\overline{N}$ that are evident in Fig. 3. However, values of ΔH

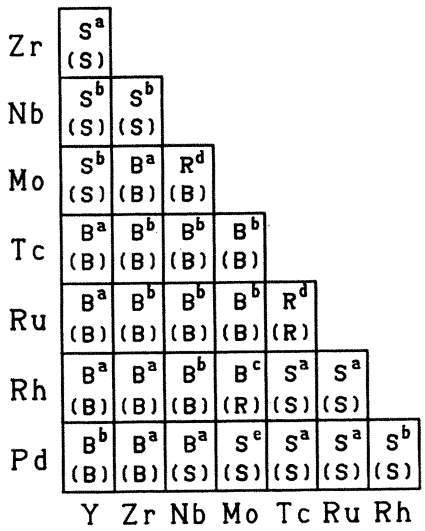

FIG. 4. Stable phase of 4*d* transition-metal alloys at $T=0$ determined from experimental phase diagrams (top) and calculated with the alloy CBLM at $x=\frac{1}{2}$ (bottom in parentheses). The letter *S* indicates that the alloy segregates, *R* indicates that the random phase is stable, and *B* indicates that the binary-ordered compound is stable. A superscript indicates the source for each experimental phase diagram and any ambiguity in interpretation: a, Ref. 68; b, Ref. 23; c, Ref. 69; d, Ref. 23, binary-ordered or segregated phase may be stable at $T=0$; e, Ref. 23, may be binary-ordered—see Ref. 69.

for specific alloys differ in magnitude and even sign from the CsCl results. Our alloy CBLM heats of formation tend to be intermediate between the CsCl and CuAu values. Of particular interest is the Nb-Mo alloy where ΔH for the CuAu structure is positive. These observations support the view that the alloy CBLM provides an accurate picture of the structure independent contribution to ΔH.

Also plotted in Fig. 3 are two experimental values[64,65] for ΔH. Both are for the random configuration, but have been compared to calculated values for the ordered compounds.[6] The measured ΔH for Rh-Pd is very close to the alloy CBLM result for the random configuration. Agreement between the measured and calculated heats of formation of Nb-Mo is not as good. This is attributed to the band-shape effect described above.

Experimental information is also available for three alloys with $\Delta N>2$ which are not included in Fig. 3. The measured[66] heat of formation of the ordered alloy PdZr is -0.64 eV/atom, and our calculated value is -0.41 eV/atom. For comparison, Moruzzi *et al.*[46] find $\Delta H=-0.50$ eV/atom for the CsCl structure and $\Delta H=-0.65$ eV/atom for the CuAu structure. Diffraction studies indicate that the actual structure is complicated.[23] The measured[67] Gibbs energy of formation of the compound RuZr in the CsCl structure is $\Delta G=-0.92$ eV/atom at 1600 K. This differs from the heat of formation by the temperature multiplied by the entropy of formation, and the pressure multiplied by the change in volume. We estimate that either term may be of order 0.05 eV/atom in magnitude. The alloy CBLM gives $\Delta H=-0.67$ eV/atom. Moruzzi *et al.* find[46] $\Delta H=-0.92$ eV/atom for the CsCl structure and -0.30 eV/atom for the CuAu structure. Finally, a bound has been placed[67] on the Gibbs energy of formation of the compound ZrRh in the CsCl structure, $\Delta G<-0.30$ eV/atom. Our calculated heat of formation is -0.87 eV/atom in agreement with this bound. Moruzzi *et al.* find $\Delta H=-0.86$ eV/atom for the CsCl structure and $\Delta H=-0.69$ eV/atom for the CuAu structure.

E. Comparison with experimental phase diagrams

Experimental phase diagrams[23,68,69] for the twenty-eight 4*d* alloys were examined to determine which of the three limiting types of SRO, segregated, random, and binary-ordered, is stable at $T=0$. The results are summarized in Fig. 4. Uncertainties in the assignments exist because of experimental variance and because experimental temperatures were often very high (>1000 °C). Alloy systems where assignments were uncertain are indicated.

Alloy systems with miscibility gaps and no compounds at low temperatures are listed as stable in the segregated phase. For alloy systems exhibiting complete solid solubility, the random phase is indicated as stable. These alloys may order or segregate below the temperatures where experimental data were taken. Alloy systems with compounds are listed as being stable in the binary-ordered phase. If the two constituents of the alloy have different elemental structures, a continuous series of solid solutions is impossible. In such cases the presence of a single compound with a large range of stable compositions at low temperatures may indicate that the random configuration is favored. The only 4*d* transition-metal alloy system whose phase diagram exhibits such a compound is Mo-Rh.

Figure 4 shows the same trends in stable phase that were seen in Fig. 3. Alloys with small or large values of $\bar{N}$ segregate and alloys for which $\bar{N}$ is near 5 form ordered compounds. Continuous solid solutions (random phase) are only found for alloys in the crossover region between segregation and binary ordering.

The stable configuration calculated from the alloy CBLM at $x=\frac{1}{2}$ is also indicated in Fig. 4. Unscreened Coulomb interactions were used. Agreement between theory and experiment is good. The only discrepancies are in the crossover region. This is the region where experimental interpretation was most uncertain and where the calculation is most sensitive to the specific choice of input parameters.[70] The three systems which do not show clear agreement are discussed below.

The alloy CBLM predicts Nb-Mo should form an ordered compound at zero temperature. However, at temperatures above about 500 K the random phase is calculated to have a lower free energy. The lowest experimental temperatures were about 1400 K so the ordered phase would not have been observed. The measured[64] random heat of formation and calculated[6] heat of formation of the CsCl structure also indicate that the ordered phase should be stable at zero temperature, and predict an order-disorder transition near 750 K.

The broad alloy phase seen in the Mo-Rh system was mentioned above. The alloy CBLM predicts that the random phase should be stable which is consistent with such a phase diagram.

The remaining discrepancy is in the Nb-Pd system. Compounds are observed at Nb concentrations of $\frac{1}{4}$ and $\frac{1}{3}$. The alloy CBLM results presented in Fig. 4 are only for $x=\frac{1}{2}$. Calculations at other concentrations show a strong asymmetry in ΔH favoring small concentrations of Nb. For the parameters given in Sec. II D the random and binary-ordered heats of formation remain positive for all concentrations. However, small changes in these parameters lead to negative random and binary-ordered heats of formation for $c_{\mathrm{Nb}}<\frac{1}{2}$ with a minimum for the binary-ordered phase near $c_{\mathrm{Nb}}=0.25$. Predictions for other alloy systems are not affected by similar changes in input parameters. Moruzzi *et al.* also found that the equiconcentration CsCl compound has a positive heat of formation.[46]

Connolly and Williams[14] have recently presented similar predictions for the 4*d* transition-metal alloys. They interpolated heats of formation calculated for several ordered compounds[46] based on the fcc structure to obtain ΔH as a function of SRO. Their predictions for the stable phase at zero temperature differ from ours for six alloy systems, Nb-Mo, Mo-Zr, Zr-Tc, Y-Tc, Tc-Ru, and Mo-Pd. In every case but the last two their results clearly disagree with available experimental data.[23,68,69] For Nb-Mo this may result from using fcc-based ordered compounds. The experimental information for Tc-Ru suggests that the random phase is stable, but does not rule out segregation at low temperatures as predicted by Connolly and Williams. Conflicting results[23,69] have been presented for Mo-Pd.

One possible explanation for the discrepancies between Connolly and William's results and experiment is that atoms are not allowed to relax about the ideal lattice sites.[46] The spacing between two "small" atoms and two "large" atoms is forced to have the same value. The energy gained by relaxing atomic positions has been considered by Froyen and Herring[71] and can be a substantial fraction of ΔH. Relaxation is included implicitly in our model because the hopping matrix elements have their elemental values—each atom retains its intrinsic volume.

V. SUMMARY AND CONCLUSIONS

The model tight-binding Hamiltonian described in Sec. II and the alloy CBLM discussed and extended in Sec. III and Appendix A provide a method for calculating the heats of formation of alloys self-consistently as a function of concentration and SRO. The only necessary input are well-defined elemental properties. The results, presented in Sec. IV and RF, are in good agreement with experiment and first-principle calculations for ordered compounds. The calculated heats of formation are consistent with the phase diagrams of twenty-seven of the twenty-eight 4*d* transition-metal alloys.

The method also provides a tool for studying the physical properties that determine the experimental trends. The contributions to the heat of formation can be understood simply in terms of the changes in valence electron DOS that are illustrated in Fig. 1. *Ionic bonding,* driven by Fermi-level differences, produces a negative contribution to ΔH. The magnitude of this contribution is strongly affected by self-consistency. *Bandwidth mismatch* decreases the strength of interspecies bonds and produces a positive contribution to ΔH. The alloys studied here contained elements with similar band structures. In other alloys the notion of bandwidth mismatch is ill-defined. The relevant factor is the relative bonding strength associated with intraspecies versus interspecies hopping. The sign of the contribution to ΔH from *band mixing,* hybridization between electronic states on different species, depends on the position of the Fermi level. It is positive when the bands are nearly full or empty, and negative when the bands are half-full. All three contributions to ΔH are included in self-consistent alloy CBLM calculations. Simpler models[8–10] were tested and found to describe at most two of these contributions accurately.

The relative magnitude of the ionic bonding, bandwidth mismatch, and band-mixing contributions to ΔH depends on the constituents of the alloy and the degree of SRO. In RF, ionic bonding and bandwidth mismatch were shown to be dominant in determining ΔH in alloys of monovalent metals. In calculations for 4*d* transition metals (Sec. IV), self-consistency reduced the contribution of ionic bonding to ΔH. The main trends in ΔH were determined by *d*-band mixing and bandwidth mismatch. These contributions increased in magnitude with changes in SRO as the number of like-neighbor bonds decreased. The free-electron bands were important in determining the stable phase of some alloys, but did not play the dominant role expected from Miedema's[7] theory.

The trends in ΔH with band filling found in the 4*d* transition-metal alloys are also seen in the phase diagrams of other alloys of transition metals (3*d*, 4*d*, and 5*d*). Exceptions are only found when the alloy contains magnetic elements and the magnetic ordering energy is large compared to ΔH. Preliminary calculations for alloys of 5*d* transition metals are in good agreement with experiment. As a general rule band mixing should be most important in alloys between elements from different columns of the Periodic Table and ionic bonding should be most important in alloys of elements from the same column.

More experimental data for heats of formation are important to test theoretical results and establish their predictive value. The strong dependence of ΔH on SRO seen in Fig. 3 points out the importance of making simultaneous measurements[25] of the degree of SRO in the alloy.

ACKNOWLEDGMENTS

We thank A. R. Williams and V. L. Moruzzi for providing band-structure results and useful discussions. Support from the National Science Foundation through Grant No. DMR-81-06494 is gratefully acknowledged. One of the authors (M.O.R.) would like to thank IBM for a fellowship during the initial phases of this research.

APPENDIX A: EXTENSION OF THE ALLOY CBLM TO THE CASE OF MULTIORBITAL BASES

The alloy CBLM was derived by Kittler and Falicov[2] based on an analogy to the CBLM for amorphous semi-

conductors.[72] Equivalent relations for a cluster of one were derived independently by Jacobs in an earlier paper.[73] Similar approximations have been considered by several authors.[74,75] For the cluster of one, a hierarchy of improved approximations can be generated. However, the alloy CBLM is exact in the limit of large coordination number,[73] and corrections are not important to the total energy or charge transfer in the systems considered here ($Z=14$).[51] They should in any event be smaller than errors associated with the approximate Bethe lattice topology.

In this appendix, the derivation of the alloy CBLM is extended to the case where there is more than one local basis orbital on each site, and there is arbitrary range hopping. In general little is gained by going beyond the first few shells of nearest neighbors. Errors associated with neglected rings of bonds become increasingly significant.

The matrix elements of the one-electron Hamiltonian can be grouped into sets associated with single sites or pairs of sites. These sets define on-site and hopping matrices whose matrix elements are

$$[\overleftrightarrow{E}_{I(i)}]_{\mu\nu}\equiv\langle i,\mu\,|\,H_{1e}\,|\,i,\nu\rangle\ , \tag{A1}$$

$$[\overleftrightarrow{t}_{I(i)J(j)}(\vec{r}_j-\vec{r}_i)]_{\mu\nu}\equiv\langle i,\mu\,|\,H_{1e}\,|\,j,\nu\rangle\ . \tag{A2}$$

The Hermiticity of the Hamiltonian implies

$$\overleftrightarrow{E}_I=\overleftrightarrow{E}_I^{\dagger}\ , \tag{A3}$$

$$\overleftrightarrow{t}_{IJ}(p,\vec{\delta})=[\overleftrightarrow{t}_{JI}(p,-\vec{\delta})]^{\dagger}\ , \tag{A4}$$

where the notation $p,\vec{\delta}$ is used in place of $\vec{r}$ to distinguish shells of neighbors related by symmetry. Each shell is labeled by the index p and contains $Z(p)$ neighbors at relative positions given by $\vec{\delta}$.

The on-site and hopping matrices are assumed to depend only on the occupation of the relevant sites. Perturbations associated with specific local environments have little effect on the total energy and are ignored. The on-site matrices, $\overleftrightarrow{E}_I$, must then be invariant under the full point group symmetry $\mathcal{G}$ of each lattice site. Each hopping matrix $\overleftrightarrow{t}_{IJ}(p,\vec{\delta})$ is invariant under the subgroup $S_{\vec{\delta}}\in\mathcal{G}$ which maps $\vec{\delta}$ into itself. Other elements of $\mathcal{G}$ take $\overleftrightarrow{t}_{IJ}(p,\vec{\delta})$ into $\overleftrightarrow{t}_{IJ}(p,\vec{\delta}')$. In general different shells have inequivalent symmetry subgroups.

For any choice of basis orbitals, representations of $\mathcal{G}$ can be constructed such that

$$\overleftrightarrow{U}_I(g)\overleftrightarrow{t}_{IJ}(p,\vec{\delta})\overleftrightarrow{U}_J^{\dagger}(g)=\overleftrightarrow{t}_{IJ}(p,\overleftrightarrow{R}_g\vec{\delta})\ , \tag{A5}$$

where $g\in\mathcal{G}$, the $\overleftrightarrow{U}_I(g)$ are unitary matrices which act on the basis orbitals, and $\overleftrightarrow{R}_g$ rotates and/or reflects the orientation vector $\vec{\delta}$. Different unitary representations, $\overleftrightarrow{U}_I(g)$, are associated with each species because their basis orbitals may differ in number, orientation, etc.

Consider an I atom on site i in the cluster which has one pth neighbor bond to a site j outside the cluster in direction $\vec{\delta}$. In the alloy CBLM the effect of this bond is replaced by a site-diagonal self-energy $\overleftrightarrow{\Sigma}_I(p,\vec{\delta})$. The value of this self-energy is calculated in the following manner.

(1) The bond connecting site i to site j is included in the cluster and all other bonds from site j are simulated with self-energies $\overleftrightarrow{\Sigma}_J(p',\vec{\delta}')$. The assumption that these self-energies are site diagonal and independent of site position relative to the cluster is only exact on a Bethe lattice.

(2) The self-energy $\overleftrightarrow{\Sigma}_I(p,\vec{\delta})$ is calculated in a mean-field approximation so that it reproduces the mean effect of site j on the matrix elements of the Green's function within the cluster. The average over possible occupations of site j includes the effect of SRO through the pair probabilities which determine the probability for finding a J atom as a pth neighbor of an I atom.

The relevant equations for the Green's function are

$$[E\overleftrightarrow{I}-\overleftrightarrow{E}_I]\cdot\overleftrightarrow{G}_{il}=\delta_{il}\overleftrightarrow{I}+\sum_{p',\vec{\delta}'}t_{IK(k)}(p',\vec{\delta}')\overleftrightarrow{G}_{kl}\ , \tag{A6}$$

$$\left[E\overleftrightarrow{I}-\overleftrightarrow{E}_J-\sum_{\vec{\delta}'(\neq-\vec{\delta}),\,p'}\overleftrightarrow{\Sigma}_J(p',\vec{\delta}')\right]\cdot\overleftrightarrow{G}_{jl}=t_{JI}(p,-\vec{\delta})\overleftrightarrow{G}_{il}\ , \tag{A7}$$

where k is the site at position $\vec{r}_i+\vec{\delta}'$, $K(k)$ is the species at site k and $\overleftrightarrow{I}$ is the identity. Solving for $\overleftrightarrow{G}_{jl}$ gives

$$[E\overleftrightarrow{I}-\overleftrightarrow{E}_I-\overleftrightarrow{\xi}_{IJ}(p,\vec{\delta})]\cdot\overleftrightarrow{G}_{il}=\delta_{il}\overleftrightarrow{I}+\sum_{\vec{\delta}'(\neq\vec{\delta}),\,p'}t_{IK(k)}(p',\vec{\delta}')\overleftrightarrow{G}_{kl}\ , \tag{A8}$$

where

$$\overleftrightarrow{\xi}_{IJ}(p,\vec{\delta})=\overleftrightarrow{t}_{IJ}(p,\vec{\delta})\left[E\overleftrightarrow{I}-\overleftrightarrow{E}_J-\sum_{p',\vec{\delta}'}\overleftrightarrow{\Sigma}_J(p',\vec{\delta}')+\overleftrightarrow{\Sigma}_J(p,-\vec{\delta})\right]^{-1}\cdot\overleftrightarrow{t}_{JI}(p,-\vec{\delta})\ . \tag{A9}$$

The self-energy for the alloy CBLM is obtained by averaging $\overleftrightarrow{\xi}_{IJ}$ over J

$$\overleftrightarrow{\Sigma}_I(p,\vec{\delta})=\sum_J\frac{y_{IJ}(p)}{c_I}\overleftrightarrow{\xi}_{IJ}(p,\vec{\delta})\ . \tag{A10}$$

Equations (A9) and (A10) specify $2\sum_p Z(p)$ coupled quadratic matrix equations for $\overleftrightarrow{\Sigma}_I(p,\vec{\delta})$. Solution of these equations can be greatly simplified through the use of group theory.

The first simplification is achieved by making the physically resonable ansatz

$$\overleftrightarrow{\Sigma}_J(p,\overleftrightarrow{R}_g\vec{\delta})=\overleftrightarrow{U}_J(g)\cdot\overleftrightarrow{\Sigma}_J(p,\vec{\delta})\cdot\overleftrightarrow{U}_J^{\dagger}(g)\ , \tag{A11}$$

for all g. Then Eqs. (A9) and (A10) reduce to

$$\overleftrightarrow{\Sigma}_I(p,\vec{\delta})=\sum_J\frac{y_{IJ}(p)}{c_I}\overleftrightarrow{t}_{IJ}(p,\vec{\delta})\cdot\left[E\overleftrightarrow{I}-\overleftrightarrow{E}_J-\sum_{p'}Z(p')\overleftrightarrow{\Sigma}_J(p')+\overleftrightarrow{\Sigma}_J(p,-\vec{\delta})\right]^{-1}\cdot\overleftrightarrow{t}_{IJ}^{\dagger}(p,\vec{\delta}) \tag{A12}$$

for any single $\vec{\delta}$ in each shell, where

$$\overleftrightarrow{\Sigma}_J(p) \equiv h^{-1} \sum_g \overleftrightarrow{U}_J(g) \cdot \overleftrightarrow{\Sigma}_J(p,\vec{\delta}) \cdot \overleftrightarrow{U}_J^{\dagger}(g) \tag{A13}$$

and h is the order of $\mathcal{G}$. The quantities $\overleftrightarrow{\Sigma}_J(p)$ are clearly invariant under the full group $\mathcal{G}$. The remainder of Eq. (A12) is invariant under $S_{\vec{\delta}}$ because $\vec{\delta}$ and $-\vec{\delta}$ lie on the same symmetry axis. The basis can be chosen to transform according to irreducible representations of $S_{\vec{\delta}}$ and thereby block-diagonalize Eq. (A12). On the bcc lattice with a basis of one s and five d orbitals, the equation for $p=1$ is reduced from a 6×6 matrix equation to two 2×2 equations. The $p=2$ equation becomes one 2×2 and three scalar equations. This represents a substantial simplification.

Evaluation of $\overleftrightarrow{\Sigma}_J(p)$ appears to require explicit representations for $U_J(g)$ and summation over all g. However, as shown below, they can be calculated trivially from partial traces of $\overleftrightarrow{\Sigma}_J(p,\vec{\delta})$. All that is needed [see (A12)] is the representation $\overleftrightarrow{U}_J(-1)$ of the element of $\mathcal{G}$ that takes $\vec{\delta}$ into $-\vec{\delta}$. If the local orbitals are eigenvectors of the inversion operator, $\overleftrightarrow{U}_J(-1)$ is a diagonal matrix with diagonal elements $+1$ and -1 for even and odd orbitals.

The basis orbitals which transform according to irreducible representations of $S_{\vec{\delta}} \in \mathcal{G}$ also transform according to irreducible representations of $\mathcal{G}$. They can be ordered so that $\overleftrightarrow{U}_J(g)$ is block diagonal

$$\overleftrightarrow{U}_J(g)_{mn} = \delta_{mn} \overleftrightarrow{u}_m(g) , \tag{A14}$$

where the indices m and n specify blocks of $\overleftrightarrow{U}$ containing matrix elements between orbitals that transform according to the mth and nth representations of $\mathcal{G}$, the $\overleftrightarrow{u}_m(g)$ are elements of the mth representation and the index J has been dropped. The matrix $\overleftrightarrow{\Sigma}_J(p,\vec{\delta})$ can be divided into rectangular blocks in the same manner

$$[\overleftrightarrow{\Sigma}_J(p,\vec{\delta})]_{mn} \equiv \overleftrightarrow{a}_{mn} . \tag{A15}$$

Equation (A13) is then

$$\overleftrightarrow{\Sigma}_J(p)_{mn} = h^{-1} \sum_g \overleftrightarrow{u}_m(g) \overleftrightarrow{a}_{mn} \overleftrightarrow{u}_n^{\dagger}(g) . \tag{A16}$$

A corollary of the great orthogonality theorem[76] states that Eq. (A16) vanishes unless m and n are equivalent irreducible representations and that if m and n are equivalent that

$$\overleftrightarrow{\Sigma}_J(p)_{mn} = C \overleftrightarrow{I} . \tag{A16'}$$

The coefficients C for the few nonvanishing blocks are calculated by noting that the trace of a matrix is invariant under unitary transformations. Thus

$$C = l_m^{-1} \mathrm{tr}(\overleftrightarrow{a}_{mn}) , \tag{A17}$$

where l_m is the dimension of the mth irreducible representation.

With the above simplifications, numerical solution of Eq. (A12) is straightforward. Guessed values of $\overleftrightarrow{\Sigma}_J(p,\vec{\delta})$ for each p and J are used to calculate $\overleftrightarrow{\Sigma}_J(p,-\vec{\delta})$, Eq. (A11), and $\overleftrightarrow{\Sigma}_J(p)$, Eqs. (A13) and (A17). Equation (A12) then gives new values for $\overleftrightarrow{\Sigma}_J(p,\vec{\delta})$. This iterative procedure converges to the physically correct solutions of (A12) for any complex energy—provided that the initial guesses for $\overleftrightarrow{\Sigma}_J(p,\vec{\delta})$ are zero. This initial condition corresponds to terminating the Bethe lattice. Convergence is slowest for energies near the van Hove singularities. These singularities are properties of the infinite system and the iteration scheme attempts to approximate them with spectral properties of a finite cluster. Convergence can be accelerated by extrapolating trends in the iterates.

For a cluster of one J atom, the diagonal element of the Green's function given by the alloy CBLM is

$$G_{00}^J(E) = \left[E\overleftrightarrow{I} - \overleftrightarrow{E}_J - \sum_p Z(p) \overleftrightarrow{\Sigma}_J(p) \right]^{-1} . \tag{A18}$$

The configuration averaged local DOS on J atoms is equal to the imaginary part of this quantity divided by π. As described in the preceding paragraph, $G_{00}^J(E)$ is most easily calculated at complex energies. However, the desired outputs of the calculation are integrals over *real* energies of the LDOS. These integrals are hard to calculate because of the van Hove singularities. An elegant way out of this dilemma is found by noting that $G_{00}^J(E)$ is analytic away from the real axis. The contour of integration can be deformed into the upper half-plane without changing the integral.[77] The value of $G_{00}^J(E)$ is easily found on this contour and the integrand is guaranteed to be smooth[78] so that numerical integration works well. In typical calculations, the convergence to solutions of (A12) on the complex contour takes $< \frac{1}{10}$ as many iterations, and $< \frac{1}{20}$ as many mesh points are needed for the numerical integration. The only trouble spots are at the points where the contour returns to the real axis. One point can be chosen below the bottom of the valence band where the LDOS is zero. The second point is the Fermi level. Numerical accuracy is reduced if this is very near a van Hove singularity.

*Present address: Exxon Research and Engineering Company, Clinton Township, Route 22 East, Annandale, NJ 08801.

[1]M. O. Robbins and L. M. Falicov, Phys. Rev. B 25, 2343 (1982).

[2]R. C. Kittler and L. M. Falicov, J. Phys. C 9, 4259 (1976).

[3]R. C. Kittler and L. M. Falicov, Phys. Rev. B 18, 2506 (1978); 19, 527 (1979).

[4]D. de Fontaine, in *Solid State Physics*, edited by H. Ehrenreich, F. Seitz, and D. Turnbull (Academic, New York, 1979), Vol. 34, pp. 73–274, and references therein.

[5]R. Kikuchi, Phys. Rev. 81, 988 (1951); R. Kikuchi and S. G. Brush, J. Chem. Phys. 47, 195 (1967).

[6]A. R. Williams, C. D. Gelatt, Jr., and V. L. Moruzzi, Phys. Rev. Lett. 44, 429 (1980), and (unpublished).

[7]A. R. Miedema, R. Boom, and F. R. de Boer, J. Less-Common Met. 41, 283 (1975); A. R. Miedema, P. F. de Châtel, and F.

R. de Boer, Physica (Utrecht) 100B, 1 (1980), and references therein.

[8]M. Cyrot and F. Cyrot-Lackmann, J. Phys. F 6, 2257 (1976).

[9]D. G. Pettifor, Phys. Rev. Lett. 42, 846 (1979); Solid State Commun. 28, 621 (1978); in *Physics of Transition Metals,* edited by P. Rhodes (Institute of Physics, London, 1981), pp. 383–391.

[10]C. M. Varma, Solid State Commun. 31, 295 (1979).

[11]R. E. Watson and L. H. Bennett, Phys. Rev. Lett. 43, 1130 (1979); Calphad 5, 25 (1981).

[12]F. Gautier, J. van der Rest, and F. Brouers, J. Phys. F 5, 1884 (1975); J. van der Rest, F. Gautier, and F. Brouers, *ibid.* 5, 2283 (1975).

[13]A. Bieber, F. Ducastelle, F. Gautier, G. Tréglia, and P. Turchi, Solid State Commun. 45, 585 (1983).

[14]J. W. D. Connolly and A. R. Williams, Phys. Rev. B 27, 5169 (1983).

[15]L. Pauling, *The Nature of the Chemical Bond,* 3rd ed. (Cornell University Press, Ithaca, New York, 1960), Chaps. 3–6.

[16]The difference in the cube root of boundary charge densities was used because Miedema found that it gave the best results.

[17]V. L. Moruzzi, J. F. Janak, and A. R. Williams, *Calculated Electronic Properties of Metals* (Pergamon, New York, 1978).

[18]J. R. Chelikowsky and J. C. Phillips, Phys. Rev. Lett. 39, 1687 (1977).

[19]J. Friedel, in *Physics of Metals: I Electrons,* edited by J. M. Ziman (Cambridge University Press, Cambridge, 1969), pp. 361–364.

[20]A. R. Williams, C. D. Gelatt, Jr., and J. F. Janak, in *Theory of Alloy Phase Formation,* edited by L. H. Bennett (AIME, New York, 1980), pp. 40–62.

[21]F. Cyrot-Lackmann, Adv. Phys. 16, 393 (1967); J. Phys. Chem. Solids 29, 1235 (1968). F. Ducastelle and F. Cyrot-Lackmann, *ibid.* 31, 1295 (1970); 32, 285 (1971).

[22]P. Soven, Phys. Rev. 156, 809 (1967); D. W. Taylor, *ibid.* 156, 1017 (1967).

[23]M. Hansen, *Constitution of Binary Alloys* (McGraw-Hill, New York, 1958); R. P. Elliot, *Constitution of Binary Alloys, First Supplement* (McGraw-Hill, New York, 1965); F. A. Shunk, *Constitution of Binary Alloys, Second Supplement* (McGraw-Hill, New York, 1969).

[24]Long-range order may be important to the heat of formation in alloys of elements with very different sizes. It plays a crucial role in determining the entropy of alloys (see Refs. 4 and 5).

[25]J. M. Cowley, Phys. Rev. 77, 669 (1950). The SRO parameter σ is directly measurable: J. M. Cowley, J. Appl. Phys. 21, 24 (1950).

[26]A Bethe lattice is a topological construct with no rings of bonds. An informative history of Bethe lattices and of calculational techniques for them is given by M. F. Thorpe, in *Excitations in Disordered Systems,* edited by M. F. Thorpe (Plenum, New York, 1982), pp. 85–107.

[27]J. C. Slater and G. F. Koster, Phys. Rev. 94, 1498 (1954); corrected and extended to higher angular momenta by R. R. Sharma, Phys. Rev. B 19, 2813 (1979).

[28]W. A. Harrison, *Electronic Structure and the Properties of Solids* (Freeman, San Francisco, 1980).

[29]V. Heine, in *Solid State Physics,* edited by H. Ehrenreich, F. Seitz, and D. Turnbull (Academic, New York, 1980), Vol. 35, pp. 1–127, and references therein.

[30]Changes with coordination number can also be important, but are not relevant in substitutional alloys.

[31]See, for example, *Electronic Structure and the Properties of Solids,* Ref. 28, pp. 47–49, 484–487.

[32]See, for example, *Electronic Structure and the Properties of Solids,* Ref. 28, pp. 52–54.

[33]L. Végard, Z. Phys. 5, 17 (1921); Z. Krist, 67, 239 (1928).

[34]Few if any alloys obey Végard's law exactly. However, deviations from it are small, on the order of a few percent (see Ref. 23).

[35]O. Kubaschewski and C. B. Alcock, *Metallurgical Thermochemistry* (Pergamon, New York, 1979).

[36]In the Hückel model, the local orbitals on each site decay exponentially. The hopping matrix elements are mostly determined by the exponential decay constants. The effective decay constant in the alloy is the *arithmetic* mean of the elemental decay constants. This implies that the hopping matrix element is given by a *geometric* mean.

[37]For small volume mismatch, this can be derived from the $\Omega^{-\alpha}$ dependence of bandwidth on volume ($\alpha=\frac{2}{3}$ or $\frac{5}{3}$) and Végard's law.

[38]F. Brouers, Ch. Holzhey, and J. Franz, in *Excitations in Disordered Systems,* edited by M. F. Thorpe (Plenum, New York, 1982), pp. 263–285.

[39]Charge fluctuations are small; see D. D. Ling and C. D. Gelatt, Jr., Phys. Rev. B 26, 2819 (1982).

[40]C. Herring, *Magnetism,* edited by G. T. Rado and H. Suhl (Academic, New York, 1966), Vol. IV, pp. 227–228. *Physics of Metals: I Electronics,* Ref. 19, pp. 376–379; J. Friedel and C. M. Sayers, J. Phys. (Paris) 38, 697 (1977).

[41]If this relation is not satisfied the elements and alloys may be unstable with respect to redistribution of charge between orbitals of different symmetry. This instability is analogous to itinerant ferromagnetism.

[42]O. K. Andersen, Solid State Commun. 13, 133 (1973); Phys. Rev. B 12, 3060 (1975); O. K. Andersen and O. Jepsen, Physica (Utrecht) 91B, 317 (1977).

[43]W. E. Pickett and P. B. Allen, Phys. Lett. 48A, 91 (1974).

[44]L. F. Mattheiss, Phys. Rev. B 1, 373 (1970).

[45]I. Petroff and C. R. Viswanathan, Phys. Rev. B 4, 799 (1971).

[46]V. L. Moruzzi, C. D. Gelatt, Jr., and A. R. Williams, *Calculated Electronic Properties of Ordered Alloys* (Pergamon, New York, 1983).

[47]C. D. Gelatt, Jr., H. Ehrenreich, and R. E. Watson, Phys. Rev. B 15, 1613 (1977).

[48]D. G. Pettifor, J. Phys. F 7, 613 (1977).

[49]S. Froyen and W. A. Harrison, Phys. Rev. B 20, 2420 (1979); S. Froyen, *ibid.* 22, 3119 (1980).

[50]L. Hodges, R. E. Watson, and H. Ehrenreich, Phys. Rev. B 5, 3953 (1972); M. Chodorow, Phys. Rev. 55, 675 (1939).

[51]M. O. Robbins, PhD. thesis, University of California, Berkeley, 1983 (unpublished).

[52]L. F. Mattheiss, Phys. Rev. 134, A970 (1964); 139, A1893 (1965); Phys. Rev. B 1, 373 (1970).

[53]D. M. Ceperley and B. J. Alder, Phys. Rev. Lett. 45, 566 (1980).

[54]Including relativistic effects or using different local density functionals, changed *differences* in d eigenvalues by 0.1 eV at most.

[55]Results of Moruzzi *et al.* (Ref. 46) suggest that a better value for the occupancy of non-d orbitals is 1.3. Atomic eigenvalues for a configuration with $1.3s$ electrons give essentially identical results to those reported in Sec. IV.

[56]In their notation $U=2u_{dd}=3.2$ eV.

[57]Values were obtained from calculated changes in s and d eigenvalues as the s or d occupation was varied.

[58]H. A. Bethe, Proc. R. Soc. London, Ser. A 150, 552 (1935).

[59]J. van der Rest, F. Gautier, and F. Brouers, J. Phys. F 5, 995 (1975).

[60]See, for example, R. Haydock, in *Solid State Physics,* edited by H. Ehrenreich, F. Seitz, and D. Turnbull (Academic, New York, 1980), Vol. 35, pp. 215–294.

[61]L. M. Schwartz, Phys. Rev. B 10, 4425 (1973).

[62]This is not formally correct. There are exponential tails in the random DOS which extend to the segregated band edges. However, the spectral weight in these tails is negligible outside the band edges given by mean-field techniques such as the CPA and alloy CBLM.

[63]N. F. Mott and H. Jones, *The Structure of Metals and Alloys* (Dover, New York, 1958); J. Friedel, Nuovo Cimento Suppl. 7, 287 (1958).

[64]S. C. Singhal and W. L. Worrell, Metall. Trans. 4, 1125 (1973).

[65]K. M. Myles, Trans. Metall. Soc. AIME 242, 1523 (1968).

[66]J. C. Gachon, J. Charles, and J. Hertz, abstract presented at the CALPHAD XII Meeting, Liege, 1983.

[67]L. Brewer and P. R. Wengert, Metall. Trans. 4, 83 (1973).

[68]W. G. Moffatt, *Handbook of Binary Phase Diagrams* (General Electric, Schenectady, New York, 1977).

[69]L. Brewer and R. H. Lamoreaux, *Atomic Energy Review, Special Issue No. 7* (International Atomic Energy Agency, Vienna, 1980), Secs. I and II.

[70]For example, different sets of on-site energies, bandwidths, or Coulomb interactions.

[71]S. Froyen and C. Herring, J. Appl. Phys. 52, 7165 (1981).

[72]J. D. Joannopoulos and M. L. Cohen, in *Solid State Physics,* edited by H. Ehrenreich, F. Seitz, and D. Turnbull (Academic, New York, 1976), Vol. 31, pp. 71–148, and references therein.

[73]R. L. Jacobs, J. Phys. F 4, 1351 (1974); 3, 933 (1973).

[74]J. Hubbard, Phys. Rev. B 19, 1826 (1979).

[75]F. Brouers, M. Cyrot, and F. Cyrot-Lackmann, Phys. Rev. B 7, 4370 (1973).

[76]M. Tinkham, *Group Theory and Quantum Mechanics* (McGraw-Hill, New York, 1964), pp. 20–25.

[77]In so doing, care must be taken not to assume analyticity of the LDOS which is just the imaginary part of an analytic function. The imaginary part of the total integral must be taken.

[78]The magnitude of the dth derivative is bounded by $|\mathrm{Im}(E)|^{-d}$.